Identifying the Uncertainty in Determining Satellite-Derived Atmospheric Motion Vector Height Attribution

Christopher S. Velden and Kristopher Bedka

Cooperative Institute for Meteorological Satellite Studies
University of Wisconsin - Madison, Wisconsin

Abstract

This study investigates the assignment of pressure heights to satellite-derived atmospheric motion vectors (AMVs), commonly known as cloud-drift and water vapor-motion winds. Large volumes of multispectral AMV datasets produced using the CIMSS/NESDIS automated algorithm are compared to collocated rawinsonde wind profiles collected by the U.S. Department of Energy Atmospheric Radiation Measurement program at three geographically-disparate sites: the U.S. Southern Great Plains, the North Slope of Alaska, and the Tropical Western Pacific. From a careful analysis of these comparisons, we estimate that mean AMV observation errors are ~5-5.5 m/s, and that vector height assignment is the dominant factor in AMV uncertainty, contributing to up to 70% of the error. These comparisons also reveal that in most cases the RMS differences between matched AMVs and rawinsonde wind values are minimized if the rawinsonde values are averaged over specified layers. In other words, on average, the AMV values better correlate to a motion over a mean tropospheric layer, rather than a traditionally assigned discrete level. The height assignment behavioral characteristics are specifically identified according to AMV height (high-cloud vs. low-cloud), type (spectral bands, clear vs. cloudy), geo-location, height assignment method, and amount of environmental vertical wind shear present. The findings have potentially important implications for data assimilation of AMVs, and these are discussed.

INTRODUCTION

The retrieval of atmospheric motion vectors (AMVs) from satellites has been evolving since the early 1970s (Schmetz et al. 1993, LeMarshall et al. 1994, Menzel 2001). Most of the major meteorological geostationary satellite data centers around the globe are now producing cloud and water vapor tracked winds with automated algorithms using imagery from operational geostationary satellites. The generally positive impact of AMVs has led to the routine assimilation, to varying degrees, in most operational global models. Contemporary AMV processing methods are continuously being updated and advanced through the exploitation of new sensor technologies, and innovative new approaches (Velden et al. 2005). Advances in data assimilation and NWP in recent years have placed an increasing demand on data quality. With remotely-sensed observations dominating the initialization of NWP models over regions of the globe that are traditionally data-sparse, the motivation is clear: the importance of providing *high-quality* AMVs becomes crucial to their relevance and contributions toward realizing superior model predictability.

AMVs are typically treated as single-level data, that is, the AMV displacements (wind speed and direction) are assigned by automated processing algorithms to a determined/estimated pressure height, and these are used by the NWP data assimilation systems. Although as noted above that AMVs have had positive impacts

on NWP, the representative vector heights have proven to be a relatively large source of observation uncertainty (Schmetz and Holmlund, 1992: Nieman et al. 1993; IWW8 2006), because in most cases the satellite imagers actually sense radiation emitted from a finite layer of the troposphere rather than just one specific level. Thus, problems in data assimilation can arise from the difficulty in accurately placing the height of the tracer, and/or representing the measured motion of a layer by a single-level value. This latter type of discrepancy is especially prevalent in clear-air WV AMVs where the radiometric signal (tracking feature) may result from a deep layer of advecting moisture (Rao et al. 2002).

The height-assignment issues discussed above, and the potential impact on NWP when assimilating AMVs, is the primary motivation for this research. Various approaches to minimize the height-assignment problems in data assimilation have been investigated, such as spreading the information over more than one level (Rao et al. 2002). However, an optimal forward operator for AMVs has remained elusive because the height assignment uncertainties and the vertical representativeness of the AMVs have not been examined thoroughly. To this end, we investigate a large and diverse sample of AMVs by comparing them with collocated rawinsondes in an attempt to determine these qualities. This information may then be exploited in numerical model simulations to determine the potential forecast impact. While the findings presented here are directly applicable only to the current NOAA/NESDIS-processed AMV datasets, they are likely also relevant to other AMV data processing centers as well, since the derivation methodologies are similar.

DATA and ANALYSIS METHODOLOGY

a. Datasets

The AMV datasets analyzed in this study are derived by the UW-CIMSS automated algorithm that is nearly identical to the code used to produce operational AMVs at NOAA/NESDIS (Daniels et al. 2002). All of the AMVs have passed the routine quality control and post-processing steps, and are considered the vectors that would be made operationally available by NESDIS to its users. Therefore, the results are robust in terms of their representativeness of NESDIS AMV datasets, and consistent with regards to the regional comparisons discussed in the next section. The AMV processing algorithm employs successive image triplets using Visible (VIS), Shortwave IR (SWIR), Water Vapor (WV), and IR Window (IRW) spectral channels. The AMV pressure-altitude assignments are derived from first passing the targeted features through a series of height assignment routines based on the radiative properties of the cloud or WV features being tracked (Nieman et al. 1993, Schmetz and Holmlund, 1992) to produce an initial set of estimated height values. Once the vector displacements are calculated, the AMVs are then passed through an automated quality control procedure (Velden et al. 1998) that can adjust the initially-assigned heights based on a best fit of each vector to a local 3-dimensional analysis of all the AMVs in the immediate vicinity (and with some influence of a model-based background analysis) and the minimization of a prescribed penalty function. In the investigations reported on in the next section, both the initial and adjusted heights are considered.

To investigate regional variations, we examine AMVs produced from both geostationary and polar-orbiting platforms (Velden et al. 2005 in diverse atmospheric conditions. The AMV datasets are compared to rawinsonde wind observations collected by the U.S. Department of Energy (DOE) Atmospheric Radiation Measurement (ARM) program at three supersites: the U.S. Southern Great Plains (SGP), the North Slope of Alaska (NSA), and the Tropical Western Pacific (TWP). The advantage in using ARM rawinsonde data is that wind observations are collected at a very high vertical resolution, every 2 seconds during the balloon flight, allowing for extra precision in the height assignment analyses described in the next section. For informational purposes, the errors in these rawinsonde winds are estimated to be ~0.5 ms^{-1} (LORAN method at SGP) and 0.2 ms^{-1} (GPS method at TWP and NSA). The

primary rawinsonde launch locations associated with these ARM sites are summarized in Table 1, in addition to the satellite instrumentation used to acquire AMVs over the three regions, the time period for the comparisons, and the total number of available AMV-rawinsonde matches.

ARM Site	Primary Sonde Launch Location(s)	Satellite Instrument(s) Used	Study Time Period	# of AMV Matches
Southern Great Plains	Lamont, OK (36.6° N 97.5° W)	GOES-12	Jan. 03-Jun. 06	6017
Tropical Western Pacific	Darwin, Australia (12.4° S, 130.9° E) Manus Island, Papua New Guinea (2.1° S, 147.4° E) Nauru Island (0.5° S, 166.9° E)	GMS-5, GOES-9, MTSAT	Jan. 03-Jun. 06	4018
North Slope of Alaska	Barrow, AK (71.3 N, 156.6 W)	Aqua and Terra MODIS	Feb. 04, Sept. 04, Oct. 04, Jul. 05, Aug. 05, May-Nov. 06	2342

***Table 1*: The primary rawinsonde launch locations associated with the indicated ARM sites, the satellite instrumentation used to acquire AMVs over the three ARM site regions, the time period for the comparisons, and the total number of available AMV-rawinsonde matches.**

b. Comparison Methodology

Each AMV data record contains the originally assigned vector altitude and the post-processed readjusted height if an adjustment was performed. We examine both of these values against collocated rawinsondes in order to assess the impact of the readjustments. The values are matched against a collocated rawinsonde at the respective AMV height assignment levels (to assess absolute accuracy), then also at the level of best rawinsonde match, or "fit" (to interrogate the accuracy possible if the height assignment error is minimized). A final component to our analysis is to examine the AMVs against layer-averaged rawinsonde values to assess the vertical representativeness of the vectors at their assigned heights, and as a further potential indicator of height uncertainty spread.

For this study, an AMV is considered for a comparison with a rawinsonde when it is matched within 50 km and one hour from the location and time of the rawinsonde launch. For each match, the AMV speed and direction is compared to the nearest (in pressure-altitude) rawinsonde value at a) the originally assigned AMV height, b) the post-processed adjusted height, c) the level of best fit (minimum vector difference within +/- 100 hPa of the assigned AMV height), and d) layer-mean rawinsonde wind values derived for layers ranging from 10 to 300 hPa in thickness starting from the assigned AMV heights. In d), rawinsonde winds are accumulated within the layer of a specified thickness, the u- and v-components are averaged, and then the vector difference between the layer-mean rawinsonde and AMV is computed. AMV-rawinsonde vector differences are further separated into categories: spectral (satellite imaging channel), height assignment level (lower tropospheric vs. upper), height assignment technique, geographic location (ARM site), local wind shear magnitude, and clear-sky versus cloudy target type (for WV AMVs). Vector root mean square (VRMS) difference statistics are computed for each of these categories.

The computations of the layer-means for d) above are done differently depending on the target type from which the AMV was derived. For clear-sky WV AMVs, the AMV height assignment represents the center of the layer-mean computations, as the signal detected by the WV channel originates from a deep atmospheric layer (Velden

et al. 1997). Thus, the layer means are computed for up to +/- 150 hPa from the assigned AMV heights. For vectors derived by cloud tracking, the AMV height assignment most closely represents the top of the cloud. Therefore, this value is used for the upper limit of the layer-mean computations, as it is assumed that a cloud target is normally advected by flow at and below cloud top (an exception to this rule is low-level tropical marine cumulus clouds (e.g., at TWP), which are often best assigned to cloud base, if that can be accurately determined). Therefore, the layer means are computed for up to 300 hPa downward from the assigned AMV heights.

c. Comparison Interpretations

The results presented in the next section are focused on the VRMS differences between the collocated AMV-rawindsonde matches. These differences should not be strictly interpreted as AMV observational error. As mentioned previously, the rawinsonde instrument measurement error is on the order of 0.2-0.5 m/s. In addition, there are errors introduced through the matching process. While our match requirements are fairly strict, any offsets in space and time can introduce an increase in the comparison differences. In order to estimate this effect in our study, two sets of comparisons were performed using ARM SGP datasets to evaluate the natural spatial and temporal variability of the local wind field. The first comparison involves the combined use of rawinsonde and 6-minute resolution wind profiler data to examine spatial variability. The wind profiler collects observations from a fixed location while the rawinsonde drifts away from the nearby profiler during ascent. Vector differences are grouped into 25 km bins based on the distance between the drifting rawinsonde and the fixed profiler locations. VRMS statistics are computed from these vector differences for each of the profiler levels at 5 distance ranges. Figure 1 presents the results of this analysis for a one year period, April 2005-2006, where data from 1626 rawinsonde ascents are included. If we assume the 0 to 25 km bin is considered a “perfect” match, the VRMS from this bin can be subtracted from the VRMS at greater bin distances at a given height to estimate the match error due to the natural spatial wind variability.

A second comparison utilizes time sequences of fixed-location 6-minute wind profiler observations to estimate the local temporal wind variability. For this analysis, a given wind profile is compared to those from 6 to 120 minutes into the future over the same one year period described above. As the profiler is in a fixed location, the vector differences between current and future wind observations are primarily related to the local temporal wind variability. For the dataset as a whole, vector differences for each successive time interval are grouped together to compute VRMS. Figure 2 shows an example of this analysis. It is assumed the VRMS difference for the initial 6-min interval is primarily caused by instrument effects and can be used as a baseline to estimate temporal wind variability at longer time intervals.

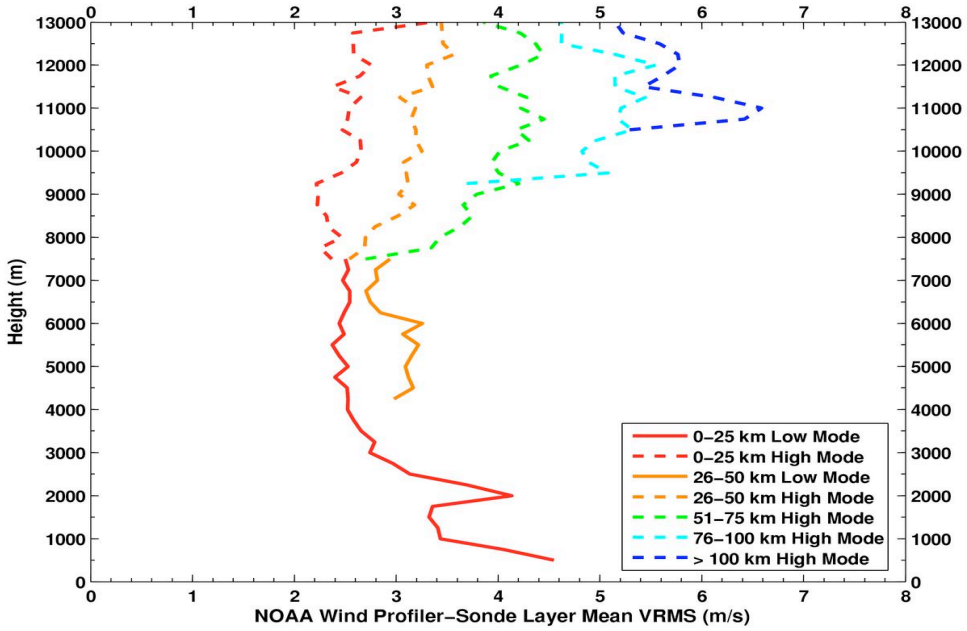

***Figure 1*: An analysis of spatial wind variability from April 2005-2006 over the ARM SGP Central Facility in Lamont, OK using fixed location 404 MHz Wind Profiler and rawinsonde observations, which are collected as the rawinsonde drifts away from the Profiler site during ascent.**

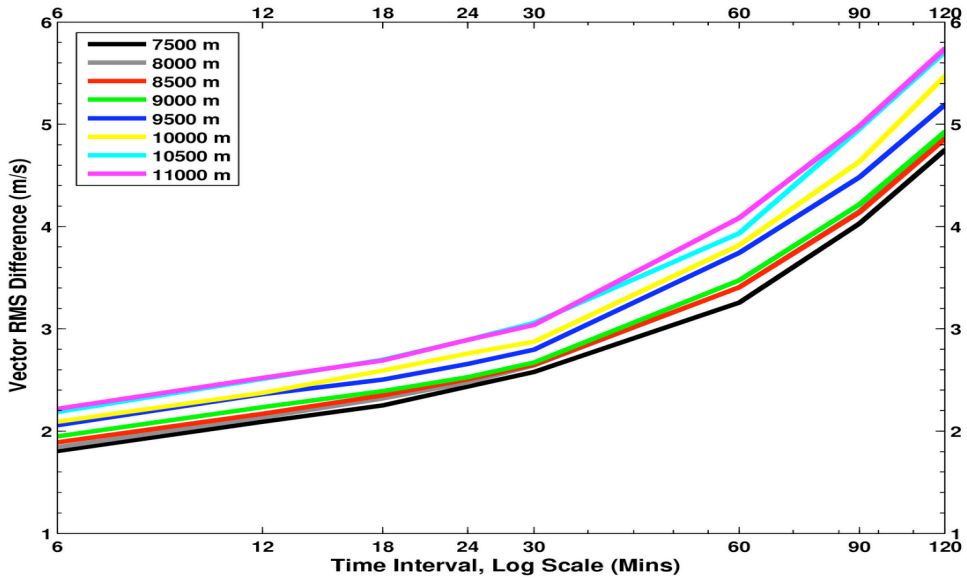

***Figure 2*: An analysis of temporal wind variability from April 2005-2006 using sequences of fixed location 404 MHz Wind Profiler observations at the SGP ARM site.**

These analyses show that the combined spatial and temporal effects on collocation "matching" statistics can be significant. These errors need to be taken into account to estimate a true AMV observation error, or in the development of a forward operator for AMVs in data assimilation. Pertinent to this study, the results presented below will estimate these errors.

RESULTS

a. Assigned AMV height level vs. rawinsonde level of best fit

To gauge the uncertainty in AMV height assignments, it is of interest to examine the characteristics of the assigned single-level AMV heights against what we will refer to as the collocated rawinsonde level of best fit (LBF). The LBF is the level of minimum AMV-rawinsonde vector difference, limited to +/- 100 hPa from the AMV height assignment (constrained to limit spurious results from rawinsonde winds far from the actual tracer height that just happen to match up the best). If we assume the rawinsonde LBF is the best possible single level wind that the AMV represents, this methodology can be used to isolate the part of AMV error associated with the uncertainty in attributing vector heights. The residual error can then be assumed to represent the aforementioned instrument and matching noise, and target tracking errors.

Tables 2a-c show the mean statistics for the collocated matches at the three ARM sites.

a)

Mean SGP Comparisons	AMV Speed (m/s)	Sonde Speed (m/s)	AMV-Sonde Speed Bias (m/s)	**AMV-Sonde VRMS (m/s)**	AMV Height (hPa)	Match Distance (km)	Time Separation (mins)
Original AMV Height	21.50	21.91	-.41	**6.31**	358	48.2	68.4
Adjusted AMV Height	22.87	23.00	-.13	**5.75**	349	48.9	69.2
Rawinsonde LBF Height	22.87	22.73	.14	**2.53**	352	49.1	69.1

b)

Mean TWP Comparisons	AMV Speed (m/s)	Sonde Speed (m/s)	AMV-Sonde Speed Bias (m/s)	**AMV-Sonde VRMS (m/s)**	AMV Height (hPa)	Match Distance (km)	Time Separation (mins)
Original AMV Height	10.21	10.68	-.47	**5.62**	271	35.1	52.2
Adjusted AMV Height	10.27	10.91	-.64	**5.27**	265	35.2	53.2
Rawinsonde LBF Height	10.27	10.09	.18	**1.96**	280	35.0	51.7

c)

Mean NSA Comparisons	AMV Speed (m/s)	Sonde Speed (m/s)	AMV-Sonde Speed Bias (m/s)	**AMV-Sonde VRMS (m/s)**	AMV Height (hPa)	Match Distance (km)	Time Separation (mins)
Original AMV Height	16.29	17.17	-.88	**5.49**	430	52.5	34.4
Adjusted AMV Height	16.30	17.19	-.89	**5.36**	430	52.5	34.5
Rawinsonde LBF Height	16.30	16.19	.12	**2.77**	444	52.2	34.5

***Table 2*: Mean comparisons between collocated AMVs and raobs at a) SGP, b) TWP, and c) NSA.**

While the VRMS statistics shown in Table 2 are not a true representation of AMV observation error, we can use this information and that gleaned in Section 2c to make a concerted estimate of this quantity, at least in terms of a mean value, as follows (Schmetz et al. (1993):

$$\textbf{Observation Error (VRMS)} = \textbf{SQRT}((\textbf{ADJ HEIGHT VRMS})^2 - (\sigma_T^2 + \sigma_S^2 + \sigma_R^2))$$

σ_T=Temporal Wind Variability (VRMS)
σ_S=Spatial Wind Variability (VRMS)
σ_R=Rawinsonde Error (VRMS)

Thus, for example at SGP, the mean VRMS is 5.7 m/s for the adjusted AMV height assignments and the mean vector height is ~350 hPa (~8300 m) from Table 2a. From this we get 1.3 m/s for the average comparison time offset, 0.3 m/s for the average spatial offset, and 0.5 m/s for rawinsonde instrument error. Applying the equation above yields an observation error (VRMS) of 5.57 m/s. While the analysis in Section 2c was based on data only from SGP, we can use it to estimate the mean AMV observational errors at the other two sites as well. The results

$$\textbf{VRMS}_{\textbf{SGP}} = \textbf{5.57 m/s}$$

$$\textbf{VRMS}_{\textbf{TWP}} = \textbf{5.12 m/s}$$

$$\textbf{VRMS}_{\textbf{NSA}} = \textbf{5.32 m/s}$$

These values are corrected for matching errors and while the adjustments are relatively small, they better represent the true bulk AMV observation errors for the three data samples.

Of particular interest to our study is the uncertainty in the AMV height assignment. This can be estimated by examining the differences in VRMS between the assigned AMV heights and the associated LBF in Table 2. In each of the three disparate regions, there is a significant reduction in the VRMS when the LBF altitude is considered as the AMV height assignment. To estimate the height attribution uncertainty, we use the following formula:

$$\textbf{Fraction of Error from Height Assignment} = 1 - \frac{\textbf{SQRT}((\textbf{LBF VRMS})^2 - (\sigma_T^2 + \sigma_S^2 + \sigma_R^2))}{\textbf{SQRT}((\textbf{ADJ HEIGHT VRMS})^2 - (\sigma_T^2 + \sigma_S^2 + \sigma_R^2))}$$

σ_T=Temporal Variability (VRMS)
σ_S=Spatial Variability (VRMS)
σ_R=Rawinsonde Error (VRMS)

Thus, after adjusting for the matching errors noted above, the height assignment uncertainty accounts for a remarkable 70% of the VRMS differences at TWP, 58% at SGP, and 49% at NSA, when compared to the original (adjusted) AMV height assignments. The reverse correlation with latitude is not surprising given the increase in tropopause height, and the greater occurrence of semi-transparent cirrus in the tropics (TWP) as AMV tracers. The latter issue has been a long-identified AMV height assignment problem area (Schmetz and Holmlund, 1992; Menzel, 2001, Nieman et al. 1993).

Having considered the height assignment uncertainty, and taking out the estimated matching error, the residual values are an indication of the error involved in the AMV targeting/tracking process. In our analysis above, these residual errors are 30%, 42%

and 51% of the total observation error for the AMVs analyzed at TWP, SGP, and NSA, respectively. The larger fraction at NSA makes sense, since the MODIS AMVs at NSA employ successive images at much greater time intervals. At SGP and TWP, the target tracking is superior due to the higher frequency of available images (Velden et al. 2005).

b. Assigned AMV height level vs. rawinsonde layer of best fit

In this section we next examine the tropospheric *layer* motion that best correlates with the AMVs. AMV-rawinsonde comparisons are plotted as VRMS differences for rawinsonde winds averaged over varying layer thickness categories (10-300hPa, in 10hPa increments, as described in section 2b), and are represented by the curves in Figs. 4-6. These analyses use AMVs from the adjusted height, with the corresponding single level-based VRMS values plotted on the y-axis. The major findings are:

- The results presented in Figs. 4-6 consistently indicate that better AMV-rawinsonde agreement exists when a layer-averaged rawinsonde wind is considered vs. just the single-level value at the assigned AMV height. The VRMS curve minima (best agreements) are on the order of 0.5 to 1 m/s lower than the corresponding single-level values. These results indicate that AMVs (at least the current NOAA/NESDIS product) are better correlated with tropospheric layer-average winds, and the optimal layer depths can be specifically identified in terms of selected AMV qualities. As mentioned previously, this result is likely a combination of AMV representativeness, and height assignment uncertainty.

- Upper-level (100-600 hPa) cloud-tracked AMVs generally correlate to a shallower layer (~30-60 hPa) than low-level tracers. Most of the upper-level tracers are cirrus clouds, which are often shallow and advect in higher shear environments. Thus, these AMVs correlate best with a shallower layer flow. TWP AMVs agree with a slightly deeper layer than those over SGP, which is likely related to differing shear characteristics, coupled with the tracking of thicker cirrus plumes associated with higher WV amounts over the tropics.

- Lower-level (600-1000 hPa) AMVs over land (SGP) best correlate to a layer depth of ~70-100 hPa. Over marine regions (TWP), these vectors better correspond to a depth of ~150-200 hPa, although the curve minima are less defined. In high latitudes (NSA), the results are less conclusive, but suggest a slight tendency to a layer thickness similar to TWP.

- Upper-level clear sky WV AMVs over all three domains agree closest with a thicker layer of ~150-250 hPa. This is not unexpected, as the signal from advecting WV features in cloud-free regions results from emittance over a thicker layer, and tracers represent layer-mean flow. This result confirms that the WV AMVs correlate best with a broad layer rather than just a single level of the troposphere.

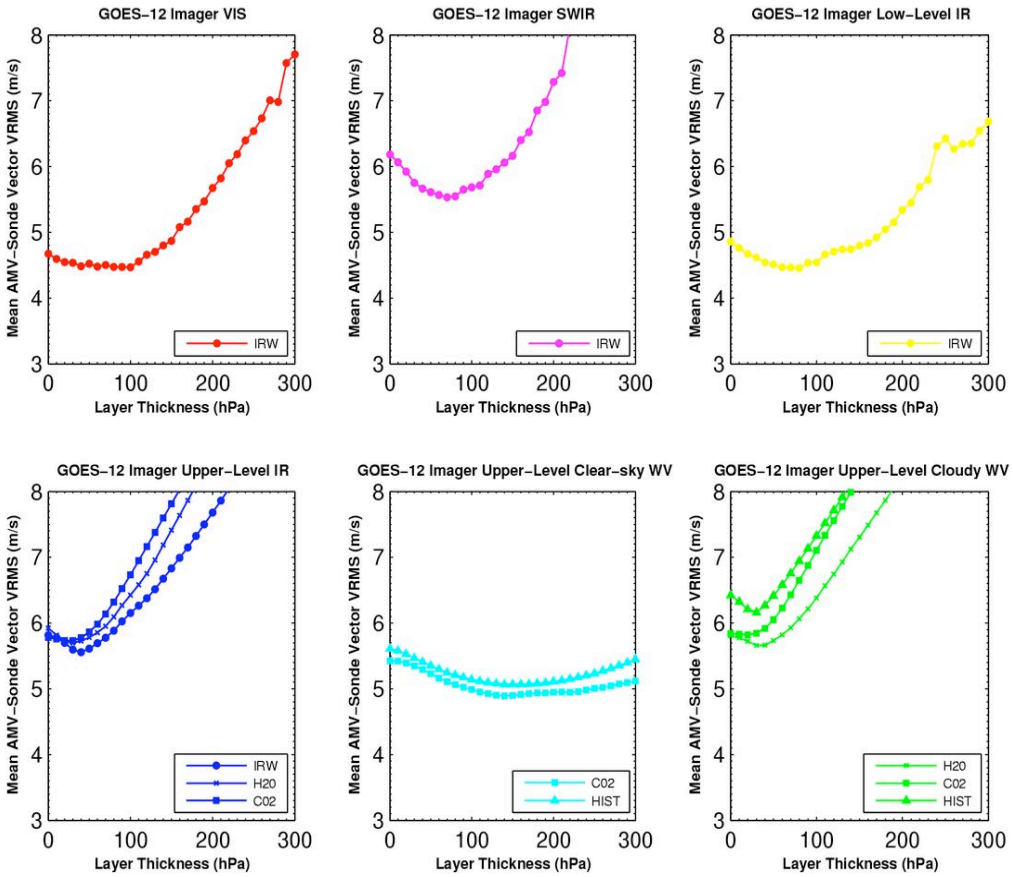

***Figure 4*: VRMS differences between GOES AMVs and layer-averaged SGP rawinsonde data for varying layer thickness (10-300hPa, in 10hPa increments) are represented by the colored curves (with the corresponding single level-based VRMS values (adjusted heights) plotted on the y-axis) for various height assignment methods: IRW – IR window method, H2O – water vapor intercept method, CO2 – CO2 slicing method, HIST – IR histogram method. The top graphs represent low-level (600-1000 hPa) AMVs from three different spectral channels: VISible, Short-Wave IR, and IR-window (long wave). The bottom graphs represent upper-level AMVs (100-600 hPa) from two different spectral channels, IR-window and 6.7 micron Water Vapor, with the WV AMVs separated by cloud vs. clear-sky targets.**

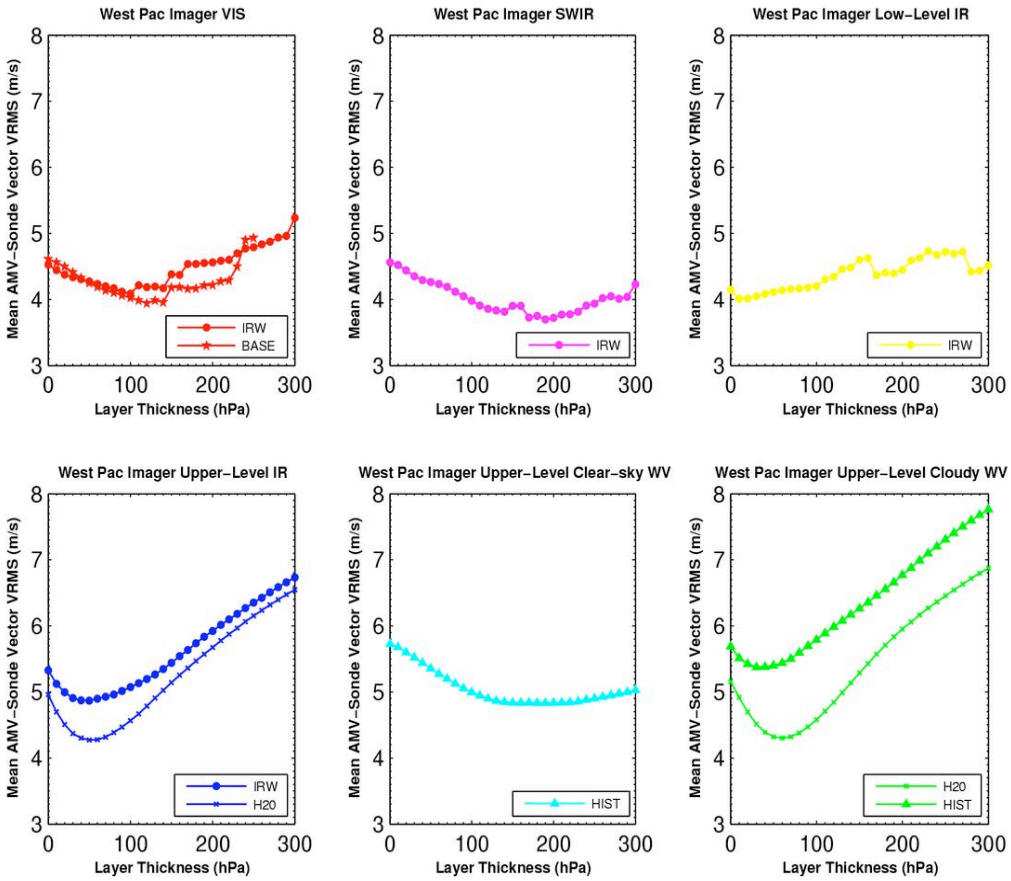

***Figure 5*: As in Fig. 4, except for AMVs derived from GMS/GOES-9/ MTSAT over the TWP ARM site.**

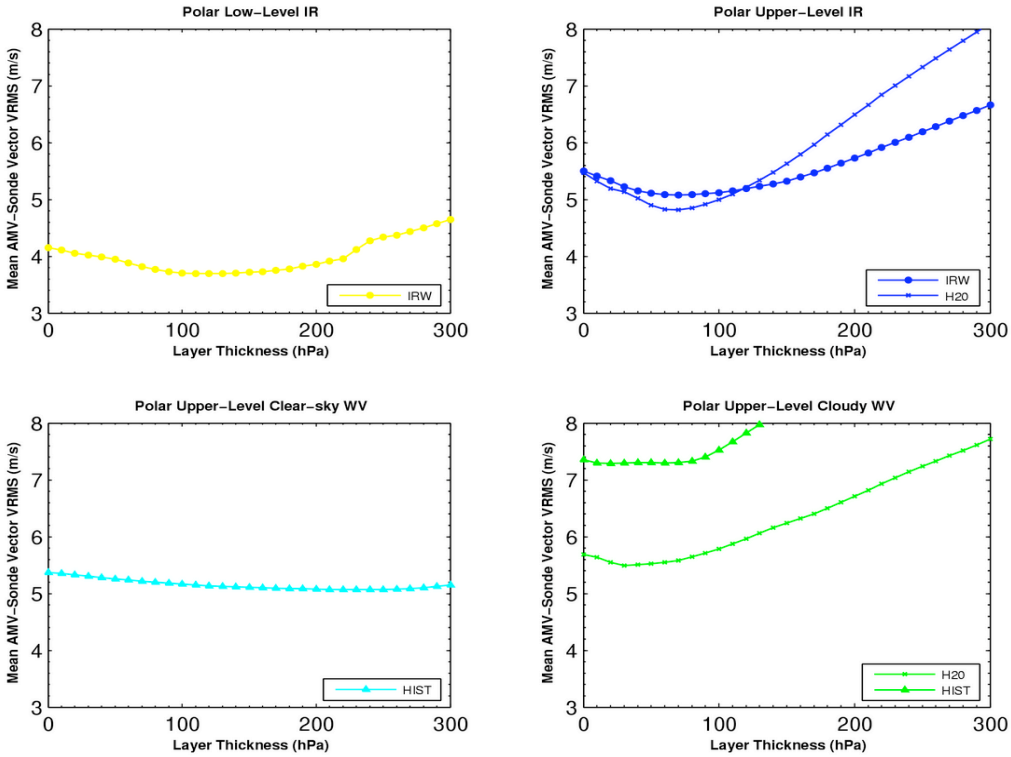

***Figure 6*: As in Figure 4, except for AMVs derived from MODIS over the NSA ARM site.**

c. Effects of vertical wind shear

The uncertainty in AMV single-level height assignments is magnified in high vertical shear environments, since even small errors can result in large misrepresentations. Analyses of AMV-rawinsonde differences with respect to varying shear regimes are shown for TPW in Figure 7. For a high shear within a low depth situation, layer-mean assignment improves agreement by up to 2-4 ms^{-1}. Similar results are found for the other two regions. In higher shear situations, the rate of VRMS increases dramatically, confirming the importance of an accurate AMV height assignment in high shear situations. These regimes appear to be the leading candidate for mitigating AMV height assignment uncertainties through layer approximations.

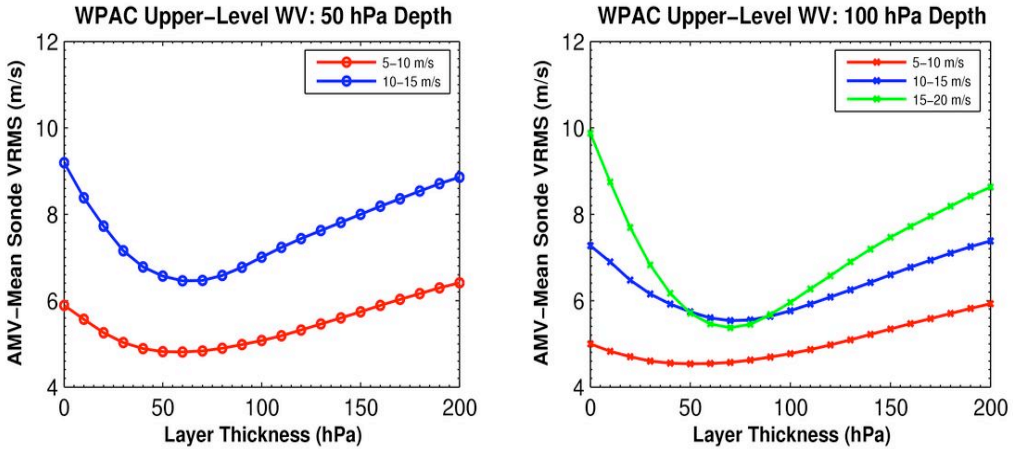

***Figure 7*: VRMS differences between cloudy upper-level WV AMVs and layer-averaged TPW rawinsonde data for varying layer thickness (10-300hPa, in 10hPa increments) are represented by the colored curves with the corresponding single level-based VRMS values plotted on the y-axis. The analyses are with respect to varying vertical wind shear regimes (curve colors). The "vertical wind shear" refers to the vector difference between the rawinsonde value at the AMV height assignment level, and two other selected rawinsonde levels (at either 50 or 100 hPa from the AMV height assignment level).**

DISCUSSION

The results found in this study strongly suggest that the uncertainty associated with height attribution is a very important contributor to AMV observation errors. Evaluation of level-based AMV height assignments indicate that significant improvements in AMV-rawinsonde vector agreements are achieved by re-assignment to a collocated rawinsonde level of 'best fit'. Since this is impractical in terms of operational applications, it is also shown that some of this height assignment uncertainty can be overcome by treating the AMVs as representing finite tropospheric *layers*, rather than single discrete levels as is currently done. Attribution of AMV information to a specified layer improves upon AMV-rawinsonde agreement by ~0.5-1 ms^{-1} over traditional level-based assignment, with significantly greater improvement (~2-4 ms^{-1}) in strong wind shear regimes. The uncertainty is likely due to a combination of vector representativeness as a finite tropospheric layer rather than discrete level, and current height assignment method inadequacies. While the results of this study only directly apply to NESDIS operational AMVs, they are likely applicable to other global data processing centers as well due to the similarities in AMV processing methodologies and quality statistics.

So how can these results be applied in NWP? Data assimilation of AMV observations could benefit by utilizing height uncertainty information, and the ancillary

information such as the optimal representative layer thickness relative to the original AMV assigned height. Future data assimilation studies should test a new AMV forward operator based on the results presented here. It is likely the most significant impact potential will be realized from regions with high shear, which would be fortuitous, since these regimes are often associated with meteorological conditions that lead to rapid model forecast error growth.

REFERENCES

Daniels, J., C. Velden, W. Bresky, A. Irving, and K. Turner, 2002: Status and development of GOES wind products at NOAA/NESDIS. *Proc. of the 6th Int. Winds Workshop,* Madison, WI, 71-80. Copies available from EUMETSAT, Am Kavalleriesand 31, D-64295, Darmstadt, Germany.

Holmlund, K., 1993: Operational water vapor wind vectors from Meteosat imagery. *Second Workshop on Wind Extraction from Operational Satellite Data,* Tokyo, Japan, EUMETSAT, 77–84.

International Winds Workshop 8, 2006. Bejing, China. Proceedings available on DVD from EUMETSAT Publications, Am Kavalleriesand 31, D-64295 Darmstadt, Germany.

Le Marshall, J.F., Pescod, N., Seaman, R., Mills, G. and Stewart, P. 1994. An Operational System for Generating Cloud Drift Winds in the Australian Region and Their Impact on Numerical Weather Prediction. *Weath. Forecasting,* **9**, 361 - 370.

Menzel, W. P., 2001: Cloud tracking with satellite imagery: From the pioneering work of Ted Fujita to the present. *Bull. Amer. Meteor. Soc.,* **82**, 33 - 47.

Nieman, S., J. Schmetz, and P. Menzel, 1993: A comparison of several techniques to assign heights to cloud tracers. *J. Appl. Meteor.,* **32**, 1559-1568.

Rao, A., C. Velden, and S. Braun, 2002: The vertical error characteristics of GOES-derived winds: Description and experiments with NWP. *J. Appl. Meteor.,* **41**, 253-271.

Schmetz, J., Holmlund, K., Hoffman, J., Strauss, B., Mason, B., Gaertner, V., Koch, A. and Van D Berg, L. 1993. Operational cloud motion winds from METEOSAT infrared images. *J. Appl. Meteor.* **32**, 1206 – 1255.

Schmetz, J., and K. Holmlund, 1992: Operational cloud motion winds from Meteosat and the use of cirrus clouds as tracers. *Adv. Space Res.,* 12 (7), 95-104.

Velden, C. S., et al., 1997: Upper-tropospheric winds derived from geostationary satellite water vapor observations. *Bull. Amer. Meteor. Soc.,* **78**, 173-195.

Velden, C. S., T. L. Olander, and S. Wanzong, 1998: The impact of multispectral GOES-8 wind information on Atlantic tropical cyclone track forecasts in 1995. Part 1: Dataset methodology, description and case analysis. *Mon. Wea. Rev.,* **126,** 1202-1218.

Velden, C., et al., 2005: Recent innovations in deriving tropospheric winds from meteorological satellites. Bull. Amer. Meteor. Soc. 86, 205-223.